Hindawi
Geofluids
Volume 2018, Article ID 9035654, 9 pages
https://doi.org/10.1155/2018/9035654

Research Article

Experimental Study on the Permeability of Weakly Cemented Rock under Different Stress States in Triaxial Compression Tests

Gangwei Fan,[1,2] Mingwei Chen,[2] Dongsheng Zhang,[1] Zhen Wang,[3] Shizhong Zhang,[2] Chengguo Zhang,[4] Qizhen Li,[2] and Bobo Cao[5]

[1]*State Key Laboratory of Coal Resources and Safe Mining, China University of Mining and Technology, No. 1 University Road, Xuzhou, Jiangsu 221116, China*
[2]*School of Mines, China University of Mining and Technology, No. 1 University Road, Xuzhou, Jiangsu 221116, China*
[3]*Research Institute of Geotechnical Engineering, Hohai University, No. 1 Xikang Road, Nanjing, Jiangsu 220098, China*
[4]*School of Mining Engineering, University of New South Wales, Sydney 2052, Australia*
[5]*Ordos Haohua Clean Coal Co. Ltd, Ordos, Inner Mongolia 017205, China*

Correspondence should be addressed to Mingwei Chen; mingwei@cumt.edu.cn

Received 10 July 2018; Accepted 30 August 2018; Published 23 October 2018

Academic Editor: Bisheng Wu

Mudstone and shaly coarse sandstone samples of Jurassic units in northwestern China were collected to study the seepage mechanism of weakly cemented rock affected by underground mining operations. Samples were studied using seepage experiments under triaxial compression considering two processes: complete stress-strain and postpeak loading and unloading. The results show that permeability variations closely correspond to deviatoric stress-axial strain during the process of complete stress-strain. The initial permeability is 7 times its minimum, contrasting with lesser differentials of initial, peak, and residual permeability. The magnitude of permeability ranges from 10^{-17} to 10^{-19} m^2, representing a stable water-resisting property, and is 1 to 2 orders lower in mudstone than that in shaly coarse sandstone, indicating that the water-resisting property of the mudstone is much better than that of the shaly coarse sandstone. Permeability is negatively correlated with the confining pressure. In response to this pressure, the permeability change in mudstone is faster than that in shaly coarse sandstone during the process of postpeak loading and unloading. Weakly cemented rock has lower permeability according to the comparison with congeneric ordinary rocks. This distinction is more remarkable in terms of the initial permeability. Analyses based on scanning electron microscope (SEM) observations and mineral composition indicate that the samples are rich in clay minerals such as montmorillonite and kaolin, whose inherent properties of hydroexpansiveness and hydrosliming can be considered the dominant factors contributing to the seepage properties of weakly cemented rock with low permeability.

1. Introduction

Underground coal mining, by default, frequently causes drastic change of primary rock stress and further triggers deformation and failure of original rocks. Under the effects of stress concentration and offloading, the permeability of rocks changes intricately along with variations in the stress state of unmodified rocks. This change can trigger engineering problems such as mine water inrush and water lose. Therefore, the variability in rock permeability under various stress states is one of the key scientific aspects from which to evaluate the impacts of coal mining on waterpower and the environment. Due to arid and semiarid conditions, as well as water shortages and a fragile environment, northwestern China is sensitive to underground mining operations, which frequently come into contact with Jurassic and Neogene formations with short diagenesis, low strength, and weak cementation, especially in Inner Mongolia, Sinkiang, Gansu, and Ningxia. Understanding the seepage characteristics of these strata under different stress conditions as well as investigating the seepage variation along different stress paths is of great significance to reduce the negative impacts of

Table 1: Specimen information and testing scheme.

Scheme	Lithology	Geological time	Buried depth (m)	Confining pressure (MPa)	Osmotic pressure (MPa)	Loading rate (mm/min)	Test content
1	Mudstone	Shuixigou group, middle-early Jurassic (J_{1-2}sh)	480	12	2	0.03	Complete stress-strain
2	Shaly coarse sandstone		490	12	2	0.03	
3	Mudstone		480	12	2	0.03	Postpeak loading and unloading
4	Shaly coarse sandstone		490	12	2	0.03	

underground coal mining on groundwater resources and flow distribution.

Research associating the permeability and seepage behavior of rocks has been performed previously, including studies of the relationship between the stress and strain and between the permeability and strain in jointed rock and brittle rock [1–4], as well as studies of the permeability variations during the process of complete stress-strain. Zhao et al. [5] and Zhang et al. [6] found that the initial permeability of jointed and brittle rock was slightly greater than its minimum, and that the maximal permeability appeared at residual stages by analyzing the permeability variation of fractured limestone, brittle limestone, medium sandstone, and fine sandstone. Experiments conducted by Wang and Xu [7] indicated that the permeability of sandstone declined sharply at residual stages and was quite different from the maximal permeability during the complete stress-strain path. Other researchers [8–10] analyzed the permeability variation behavior of cracked and brittle rock under different experimental conditions, including confining pressure, osmotic pressure, pore pressure, and loading-unloading pressure. As a result, Billiotte et al. [11] and Wong et al. [12] found that the permeability of brittle mudstone, sandstone, jointed sandstone, and siltstone decreased as the confining pressure increased. Li et al. [13] found that the impacts of confining pressure and pore pressure on the permeability of sandstone were notable during the postpeak phase but were less substantial during the prepeak phase. The gas permeability variation of sandstone samples under confining pressure was also studied by Wang et al. [14], who indicated that gas permeability was greater after unloading than before loading and was greater during the process of loading than during unloading under an equivalent confining pressure. In addition, stress, seepage, and temperature have been coupled in studies [15] of the permeability variation law under more complicated practical conditions. Meng et al. [16] and Ding et al. [17] found that the permeability of phyllite and cracked sandstone decreased with increasing temperature within a limited scope, but increased when temperature exceeded a certain value. Simultaneously, increasing the confining pressure resulted a decreasing impact of temperature on the permeability of cracked sandstone.

Currently, the basic variation law of rock permeability under different conditions can be acquired through the above method; however, few studies have examined rock samples collected from a formation with weak cementation. For the rock hosted in the Jurassic formation in northwestern China or its congener with short diagenesis, weak cementation, and low strength, further study of the factors governing the variation of permeability is required.

This paper, based on previous studies, collects mudstone and shaly coarse sandstone from the Jurassic weak cementation formation hosted in the Laosangou coal mine in Inner Mongolia as samples to test permeability under triaxial compression utilizing an MTS815 tester. Additionally, the microstructure and mineral composition are investigated. The results show that mudstone and shaly coarse sandstone are weakly cemented and have developed voids and loose structure. These samples are rich in clay minerals, including kaolin, illite, and montmorillonite, which have the characteristics of swelling and mudding during encounters with water. These analyses help reveal the seepage properties of weakly cemented mudstone and shaly coarse sandstone and can provide practical information for engineering projects.

2. Methods

Underground coal mining would grant original rock with plastic zones, where most rock has transitioned to postpeak phase, but the rock outside such zones could undergo the process of complete stress-strain. Therefore, by focusing on such rock samples, the experiments in this paper mainly study the variability in permeability during processes of complete stress-strain as well as postpeak loading and unloading. In addition, the horizontal stress of plastic softening zone and plastic residual zone averages 50 to 80 percent of primary rock stress. So, unloading pressures with rates of 0.5γH and 0.75γH are employed to emulate stress states of rock mass in different plastic zones during the process of postpeak loading and unloading.

Based on the transient method, typical mudstone and shaly coarse sandstone samples were collected from the weak cementation formation of the Jurassic and were tested using the electrohydraulic servo system to determine the permeability during the processes of complete stress-strain as well as postpeak loading and unloading. According to the results of experiments, the variability of permeability under different stresses and confining pressures was analyzed.

2.1. Experimental Scheme. Each rock core was collected from an in situ borehole at the Laosangou coal mine in Inner Mongolia and was then standardized to be suitable for seepage experiments in the laboratory. After soaking in water, samples were tested by controlling the constant loading rate and osmotic pressure difference. The confining pressure should be 12 MPa based on the sampling depth of 500 m.

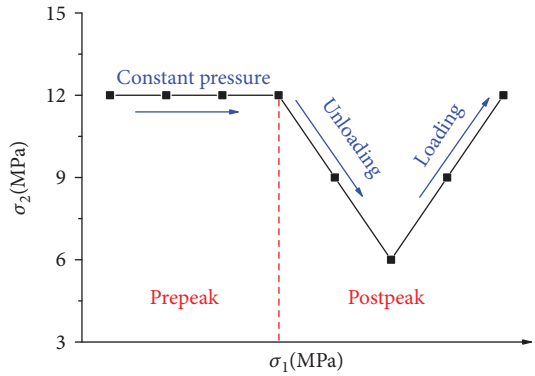

FIGURE 1: Stress path of samples during the process of postpeak loading and unloading of confining pressure.

Next, two scenarios, including complete stress-strain and postpeak loading and unloading, were designed to investigate the permeability variation in the rock samples. Information on the preparation and testing parameters for the rock samples is shown in Table 1.

2.2. Testing Methods. During the process of complete stress-strain, the confining pressure was adjusted to 12 MPa first to simulate the stress state of virgin rocks. The initial permeability could be measured under hydrostatic pressure. Then, an axial stress was applied by maintaining displacement, during which the dynamic permeability was recorded until the residual strength phase.

During the process of postpeak loading and unloading, pretreatment resembling that used in previous studies was conducted. A confining pressure of 12 MPa was maintained to simulate the stress state of virgin rocks. After the residual strength phase, the permeability was recorded while maintaining a constant loading rate and reducing the confining pressure from 12 MPa (γH) to 9 MPa (0.75 γH) to 6 MPa (0.5 γH) and then increasing the confining pressure to 9 MPa (0.75 γH) and then 12 MPa (γH), all a rate of 3.75×10^{-2} MPa/min. The stress path of this process is shown in Figure 1.

3. Results

The permeability variation in rock samples during the two processes could be acquired by conducting permeation tests under triaxial compression. The results are as follows.

3.1. Process of Complete Stress-Strain. The test results for the permeability of weakly cemented mudstone and shaly gritstone during the process of complete stress-strain are shown in Figure 2.

Observations of the failure modes (Figure 2) reveal that the mudstone sample appears to have a compact structure and few impurities, whereas large particle fillers are visually observed in the shaly coarse sandstone. Furthermore, the mudstone sample has experienced obvious plastic deformation. For the sample of shaly coarse sandstone, after testing, the main fracture sloped from the bottom upward.

Figure 2 presents the changes between the deviatoric stress, permeability, and axial strain of two types of samples during the entire process of complete stress-strain. Three stages, including the consolidation and elastic stage, yield stage, and residual stage, could be defined to describe the permeability variation during the entire process of complete stress-strain. For both weakly cemented mudstone and shaly coarse sandstone samples, in the first stage, there was a gradual decrease in permeability until the minimum was reached. At the beginning of the second stage, the permeability rapidly increased until it reached the maximum and then slightly decreased during the third stage, when the permeability was approximately equal to the peak value. The permeabilities of both samples were less than 10^{-17} m^2, which indicates that the rock has a low penetrability and strong water-resisting properties. Additionally, mudstone has a stronger impermeability because its permeability is 2 orders of magnitude less than that of shaly coarse sandstone.

In this paper, k_{min}, k_0, k_{ave}, and k_{max} are the minimum permeability, initial permeability, average permeability during the residual stage, and maximum permeability of weakly cemented mudstone and shaly coarse sandstone, respectively. Through comparison, k_0 is slightly different from k_{max} and k_{ave} and substantially different from k_{min}. Specifically, the k_0 values of both samples are 6.717 and 7.546 times their k_{min}. Besides, k_{max} values are 1.211 and 1.787 times k_0, and k_{ave} values are 1.065 and 1.769 times k_0. The permeabilities of weakly cemented mudstone and shaly coarse sandstone at each stage are summarized in Table 2.

3.2. Process of Postpeak Loading and Unloading. The curve of deviatoric stress and permeability with axial strain increases during the entire process of postpeak loading and unloading is shown in Figure 3.

For mudstone samples, Figure 3(a) shows that the permeability steadily increases from around 6.3×10^{-19} m^2 to 1.05×10^{-18} m^2 with the confining pressure unloading from 12 MPa to 6 MPa, yet dramatically decreases to 7.0×10^{-19} m^2 then to 6.8×10^{-19} m^2 with the confining pressure proceeding to load, whereas the permeability of shaly coarse sandstone samples sees a different evolution characteristic. It can be seen in Figure 3(b) that, after a significant increase from 6.8×10^{-19} m^2 (12 MPa) to around 8.6×10^{-19} m^2 (6 MPa) with confining pressure unloading, the permeability keeps increasing to 9.4×10^{-19} m^2 with confining pressure growing by 3 MPa, then falls back to less than 8.0×10^{-19} m^2 (12 MPa).

In terms of the holistic evolution characteristics, as shown in Figure 3, the permeability of weakly cemented rock is significantly affected by and is negatively correlated with the confining pressure. For the mudstone sample, the permeability sensitively appears synchronous variation with confining pressure. The permeability variation is hysteretic when it occurs in the shaly coarse sandstone sample. During the process of unloading the confining pressure, the permeability increases slightly when the confining pressure decreases from 12 MPa to 9 MPa and greatly decreases when the confining pressure further increases from 9 MPa to 12 MPa. When the confining pressure increases, the permeability exhibits the opposite trend to that when the confining

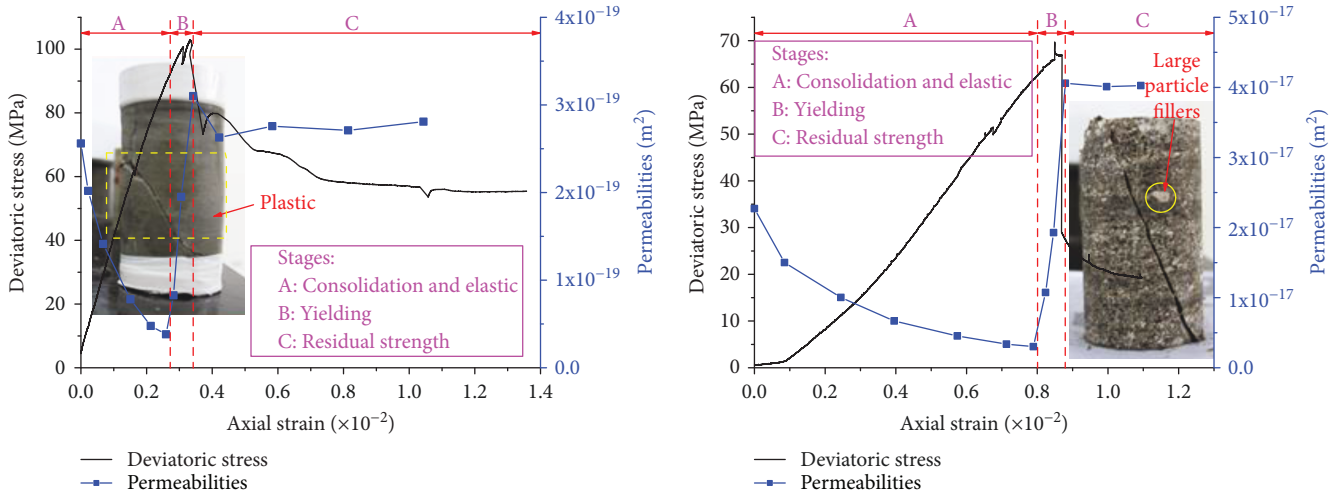

Figure 2: Variations in the permeability of weakly cemented rock during the process of complete stress-strain.

Table 2: Summary of rock permeabilities in different stages during the process of complete stress-strain.

Lithology	k_0 (m^2)	k_{min} (m^2)	k_{max} (m^2)	k_{ave} (m^2)	Ratio $\frac{k_0}{k_{min}}$	Ratio $\frac{k_{max}}{k_0}$	Ratio $\frac{k_{ave}}{k_0}$
Mudstone	2.5607×10^{-19}	3.8128×10^{-20}	3.1005×10^{-19}	2.7261×10^{-19}	6.717	1.211	1.065
Shaly coarse sandstone	2.2712×10^{-17}	3.0099×10^{-18}	4.0595×10^{-17}	4.0181×10^{-17}	7.546	1.787	1.769

pressure decreases. These analyses indicate that a lower confining pressure can greatly affect rock permeability during the entire process of postpeak loading and unloading.

After loading and unloading is completed, the permeability at the stage of termination is slightly higher than the original permeability. Specifically, the final permeabilities of mudstone and shaly coarse sandstone are 1.082 and 1.084 times the permeabilities before loading and unloading, respectively. Compared with the initial permeability, the final permeability is 1.158 and 2.153 times greater for mudstone and shaly coarse sandstone, respectively. Mudstone, whose permeability is 1 order of magnitude less than that of shaly coarse sandstone, has a stronger water-resisting property. The permeabilities at each stage of postpeak loading and unloading are summarized in Table 3.

4. Discussion

Based on the above results of seepage experiments, this paper finds that the permeability characteristics of weakly cemented rocks are obviously different from that of common rocks. Other kinds of common mudstone and sandstone are selected to make comparison, whose permeability curves are demonstrated in Figure 4. Specifically, three indicators including the initial permeability, the minimum permeability, and the peak permeability can be utilized to reveal the differences between permeability characteristics of weakly cemented rocks and others. Based on the seepage experiments on mudstone specimen conducted by Liu et al. in 2015 [18], it can be seen firstly in Figure 4(a) that the permeability of weakly cemented mudstone is obviously lower than common mudstone because of the disparity in 2 orders of magnitudes. In addition, from a certain initial value, the permeability of common mudstone slightly drops to the minimum, and yet dramatically soars to the peak, which is approximately 6 times the initial, whereas the permeability curve of weakly cemented mudstone sees a completely different characteristic. There is only a small gap between the initial permeability and the peak, whose values are much bigger than the minimum. As for the sandstone, Figure 4(b) indicates that there is a relatively small difference between the initial permeability and the peak permeability of weakly cemented sandstone, and the permeabilities of weakly cemented sandstone are just slightly less than that of common sandstone tested by Zhang et al. in 2013 [6]. During the process of complete stress-strain, the initial permeability common sandstone is just 1 to 2 times the minimum, but dramatically is less than that of the maximum permeability, whose value is even 50 times that of the former.

In light of the abovementioned comparison, the rocks with weak cementation have lower permeabilities during the whole process of complete stress-strain than other kinds of common rocks. Furthermore, its permeability characteristics are starkly different as well. Therefore, in order to explore the factors that cause such permeability characteristics of weakly cemented rocks and to investigate whether there is a correlation between the seepage properties and the microstructures and compositions, further researches revolving around the microstructure and composition should be

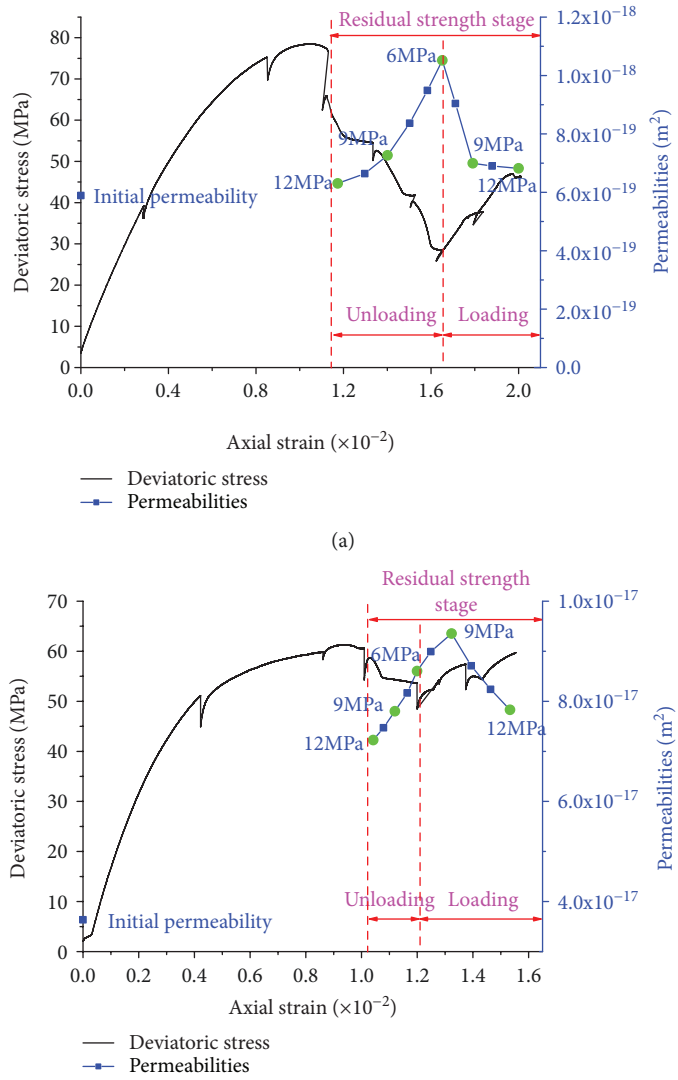

Figure 3: Variations in the permeability of weakly cemented rock during the process of postpeak loading and unloading.

Table 3: Summary of the permeabilities of rocks in different stages during the process of postpeak loading and unloading.

Lithology	k_0 (m^2)	k_1 (m^2)	k_2 (m^2)	Ratio $\frac{k_2}{k_1}$	Ratio $\frac{k_2}{k_0}$
Mudstone	5.8889×10^{-19}	6.3035×10^{-19}	6.8219×10^{-19}	1.082	1.158
Shaly coarse sandstone	3.6364×10^{-18}	7.2248×10^{-18}	7.8290×10^{-18}	1.084	2.153

launched using a scanning electron microscope (SEM) and X-ray diffraction (XRD), respectively.

4.1. Effects of Microstructures. In recent years, SEM has been endowed increasingly expensive applications on investigating the microstructures within the natural rock mass [19]. The SEM results of weakly cemented mudstone and shaly coarse sandstone are shown in Figure 5.

At an amplification of 2000 times, abundant structures such as flocculent kaolin and flaky illite were observed, as shown in Figure 5(a). Flocculent fillers similar to kaolin also existed in the voids of shaly coarse sandstone, as shown in Figure 5(b). After turning up the amplification to a factor of 8000, voids developed in the inner mudstone and shaly coarse sandstone. These voids indicate that clay minerals such as kaolin and illite exist in two types of observed states, which also have loose structures, have developed voids, and are weakly cemented. Both minerals have been observed to exhibit considerable swelling and mudding when encountering water [20, 21]. This response may be a primary factor contributing to the low permeabilities of less than 10^{-17} m^2 of mudstone and shaly coarse sandstone as well as their

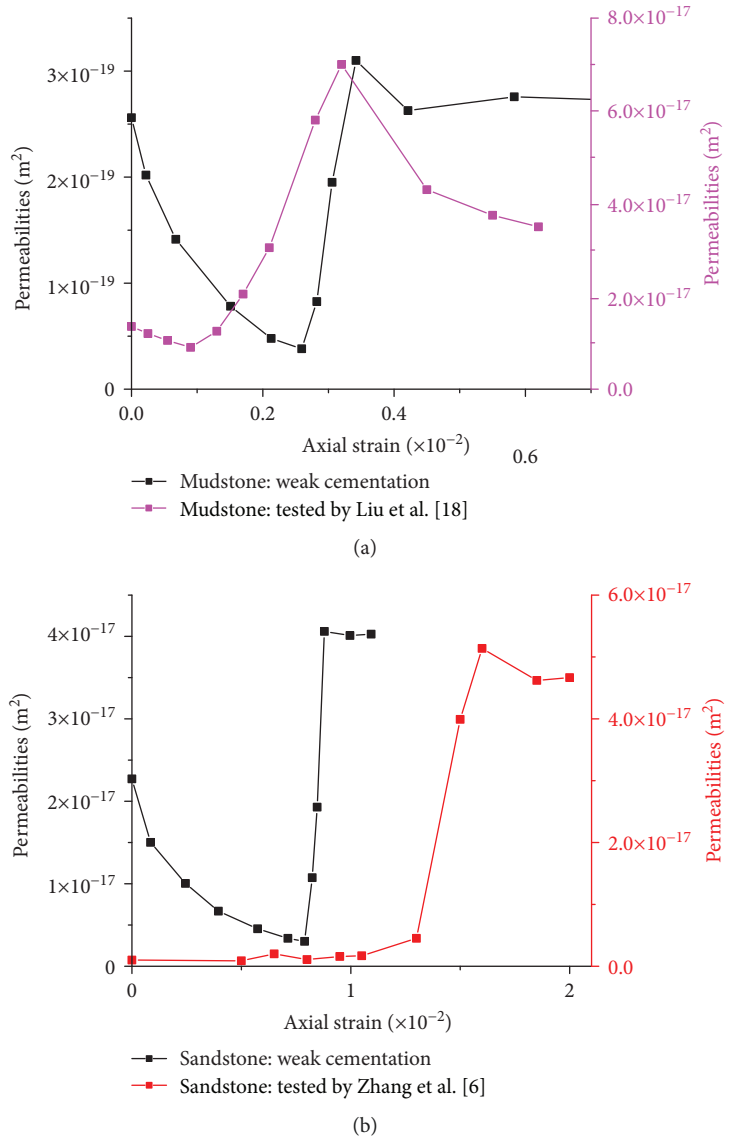

Figure 4: Permeability comparisons of weakly cemented rocks with common rocks of mudstone and sandstone, respectively.

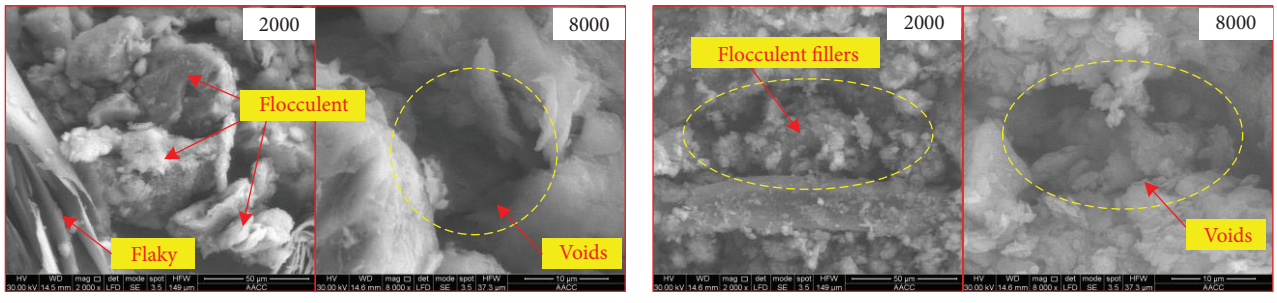

Figure 5: Microstructures of specimens obtained using SEM at different magnifications.

strong water-resistant properties. However, loose structures and voids cause rock to compress, causing the initial permeability of both samples to be 7 times the minimum during the process of complete stress-strain.

4.2. Effects of Mineral Compositions. XRD was utilized to analyze the composition of weakly cemented mudstone and shaly coarse sandstone; the diffraction patterns of which are shown in Figure 6.

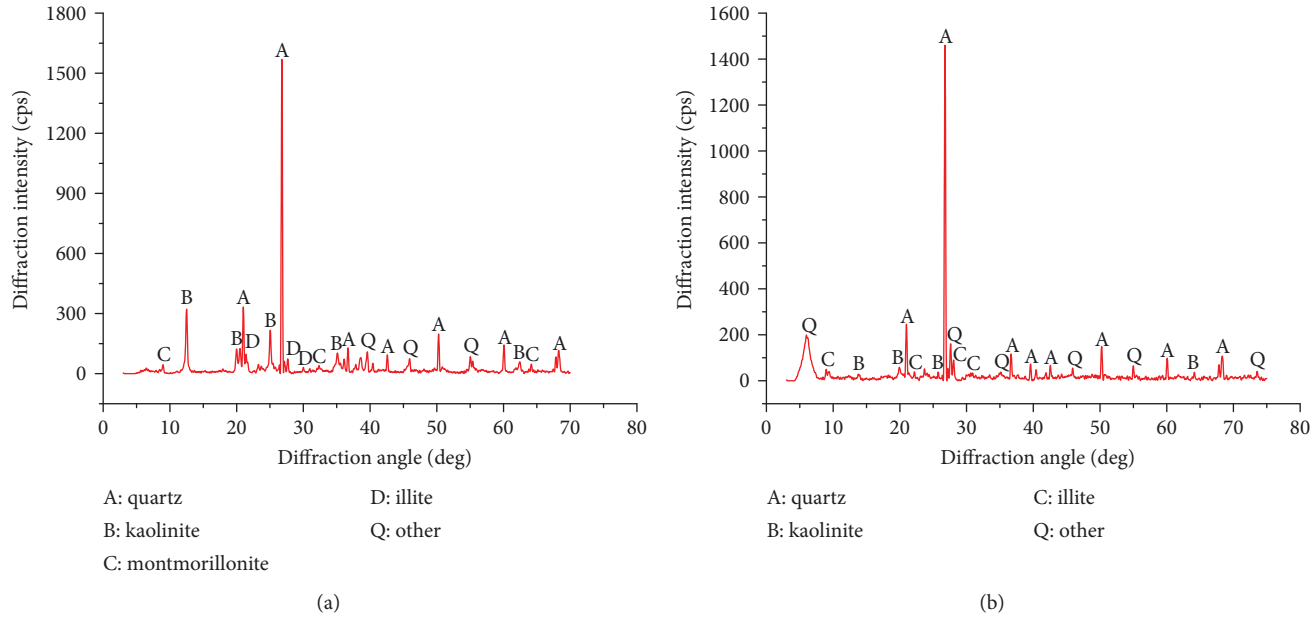

Figure 6: X-ray diffraction patterns of specimens.

Table 4: Results of composition analysis in specimens using X-ray.

Lithology	Quartz (%)	Kaolin (%)	Montmorillonite (%)	Illite (%)	Other (%)	Clay minerals (%)
Mudstone	73.13	15.09	2.24	4.56	4.98	21.89
Shaly coarse sandstone	79.90	4.50	—	6.15	9.45	10.65

The results of XRD show that mudstone contains abundant clay minerals such as kaolin, montmorillonite, and illite, while shaly coarse sandstone mainly contains kaolin and illite. The contents of clay minerals in the two samples are listed in Table 4. Specifically, quartz occupies the highest content in mudstone and shaly coarse sandstone, with concentrations of 73.13% and 79.90%, respectively, followed by clay minerals, with percentages of 21.89% and 10.65%, respectively. The primary compositions of clay minerals in mudstone are kaolin, montmorillonite, and illite with percentages in total clay minerals of 15.09%, 2.24%, and 4.56%, respectively. The primary compositions of clay minerals in shaly coarse sandstone are kaolin and illite, with concentrations in total clay minerals of 4.50% and 6.15%, respectively. By comparison, clay minerals in mudstone are 2.06 times more abundant than that of those in shaly coarse sandstone.

Compared to shaly coarse sandstone, mudstone has more types and contents of clay minerals, which might be the main reason that the permeability of mudstone was one to two orders of magnitude lower than that of shaly coarse sandstone in different tests. Similarly, the results of the composition test show that the permeability of weakly cemented rock is inversely proportional to the clay mineral content.

The permeability variation of weakly cemented mudstone and shaly coarse sandstone during the process of complete stress-strain can be described as follows. During the consolidation and elastic stages, natural voids that existed in the samples are gradually consolidated and new fractures have not yet been generated. Therefore, the permeability gradually decreases at a rate that is significantly faster in the consolidation stage than in the elastic stage. The permeability reaches a minimum at the end of the elastic stage. During the yield stage, the permeability increases rapidly, with new fractures gradually developing. Simultaneously, new fractures develop most fully as the stress reaches a peak, and permeability also rises to its maximum value. During the residual stage, fractures continue to develop, and previously generated fractures may begin to close. Additionally, after encountering water, clay minerals such as kaolin and illite in the samples may swell and turn to mud, which could plug some seepage channels. Under the combined action of these factors, the permeabilities of weakly cemented mudstone and shaly coarse sandstone reach their peak values.

5. Conclusion

Based on the weakly cemented mudstone and shaly coarse sandstone samples from the Jurassic in northwestern China, permeability is tested via two types of processes: complete stress-strain and postpeak loading and unloading. A general variation law governing the permeability of weakly cemented rock is identified. The results of SEM and XRD analyses show that the seepage property is closely related to the microstructures and compositions of rock, and the relationship has been briefly analyzed here.

The seepage experiments under triaxial compression indicate that the permeability of weakly cemented rock has distinctive characteristics. During the process of complete stress-strain, the permeability gradually decreases at the elastic stage till reaching the minimum. Then, it rapidly increases to the maximum at the end of the yield stage, following by a slight decrease at the residual stage, during which it reaches and remains the peak. The initial permeability is 7 times its minimum, contrasting with lesser differentials of initial, peak, and residual permeability. The permeability ranges from 10^{-17} to 10^{-19} m^2, representing a stable water-resisting property. Mudstone owns better water resistance according that its permeability is 1 to 2 orders of magnitude lower than shaly coarse sandstone. A negative correlation exists between permeability and confining pressure, and therefore, the permeability variation in mudstone is faster than that in shaly coarse sandstone during the process of postpeak loading and unloading.

The results of SEM and XRD show that rock samples developed voids and loose, weakly cemented structure. Moreover, such clay minerals as kaolin, montmorillonite, and illite are abundant. Analysis indicates that some natural compression spaces may be the reason that the initial permeability is approximately 7 times the minimum permeability during the process of complete stress-strain. Besides, clay minerals endow samples with strong water resistance because of the swelling and mudding characteristics while encountering water. During the residual stage, these characteristics also allow fractures to continue developing; meanwhile, previously developed fractures may begin to close so that the permeability remains approximately constant. Compared to shaly coarse sandstone, there are more clay minerals in mudstone but with lower permeability, which indicates that permeability is inversely proportional to the clay mineral content.

Data Availability

The data of this manuscript is tested in the laboratory of State Key Laboratory of Coal Resources and Safe Mining, China University of Mining and Technology, which is available to authorized users.

Conflicts of Interest

The authors declare that they have no conflicts of interest.

Acknowledgments

This research was financially supported by the National Natural Science Foundation of China (Grant no. 51504240), the National Key Basic Research Program of China (973 Program) (Grant no. 2015CB251600), the Fundamental Research Funds for the Central Universities (Grant no. 2017XKZD07), the Jiangsu Basic Research Program (National Natural Science Foundation of China) (Grant no. BK20150051), the State Key Laboratory of Coal Resources and Safe Mining (Grant no. SKLCRSM18X007) and the Qinglan Project in Jiangsu Province of China (Grant no. [2016] 15).

References

[1] D. T. Snow, "Fracture deformation and changes of permeability and storage upon changes of fluid pressure," *Q J Colorado School Mines*, vol. 63, no. 1, pp. 201–244, 1968.

[2] N. G. W. Cook, "Natural joints in rock: mechanical, hydraulic and seismic behaviour and properties under normal stress," *International Journal of Rock Mechanics and Mining Sciences & Geomechanics Abstracts*, vol. 29, no. 3, pp. 198–223, 1992.

[3] M. Oda, "An equivalent continuum model for coupled stress and fluid flow analysis in jointed rock masses," *Water Resources Research*, vol. 22, no. 13, pp. 1845–1856, 1986.

[4] J. Heiland, "Laboratory testing of coupled hydro-mechanical processes during rock deformation," *Hydrogeology Journal*, vol. 11, no. 1, pp. 122–141, 2003.

[5] Y. Zhao, J. Tang, Y. Chen et al., "Hydromechanical coupling tests for mechanical and permeability characteristics of fractured limestone in complete stress–strain process," *Environmental Earth Sciences*, vol. 76, no. 1, 2017.

[6] R. Zhang, Z. Jiang, Q. Sun, and S. Zhu, "The relationship between the deformation mechanism and permeability on brittle rock," *Natural Hazards*, vol. 66, no. 2, pp. 1179–1187, 2013.

[7] H. Wang and W. Xu, "Relationship between permeability and strain of sandstone during the process of deformation and failure," *Geotechnical and Geological Engineering*, vol. 31, no. 1, pp. 347–353, 2013.

[8] D. Ma, X. X. Miao, Z. Q. Chen, and X. B. Mao, "Experimental investigation of seepage properties of fractured rocks under different confining pressures," *Rock Mechanics and Rock Engineering*, vol. 46, no. 5, pp. 1135–1144, 2013.

[9] Z. Liu and D. Jin, "Experimental research of rock strength and permeability characteristics under different confining and hydraulic pressure," in *12th International Mine Water Association Congress (IMWA 2014): An Interdisciplinary Response to Mine Water Challenges*, pp. 183–186, Xuzhou, China, 2014.

[10] X. Liu, J. Liu, N. Liang, C. He, Z. Zhong, and B. Zeng, "Experimental and theoretical analysis of permeability characteristics of sandstone under loading and unloading," *Journal of Engineering Science and Technology Review*, vol. 9, no. 5, pp. 36–43, 2016.

[11] J. Billiotte, D. Yang, and K. Su, "Experimental study on gas permeability of mudstones," *Physics and Chemistry of the Earth, Parts A/B/C*, vol. 33, Supplement 1, pp. S231–S236, 2008.

[12] L. N. Y. Wong, D. Li, and G. Liu, "Experimental studies on permeability of intact and singly jointed meta-sedimentary rocks under confining pressure," *Rock Mechanics and Rock Engineering*, vol. 46, no. 1, pp. 107–121, 2013.

[13] S. P. Li, D. X. Wu, W. H. Xie et al., "Effect of confining presurre, pore pressure and specimen dimension on permeability of Yinzhuang sandstone," *International Journal of Rock Mechanics and Mining Sciences*, vol. 34, no. 3-4, pp. 175.e1–175.e11, 1997.

[14] H. L. Wang, W. Y. Xu, M. Cai, Z. P. Xiang, and Q. Kong, "Gas permeability and porosity evolution of a porous sandstone under repeated loading and unloading conditions," *Rock Mechanics and Rock Engineering*, vol. 50, no. 8, pp. 2071–2083, 2017.

[15] S. Olivella, A. Gens, and C. Gonzalez, "THM analysis of a heating test in a fractured tuff," in *Coupled Thermo-Hydro-Mechanical-Chemical Processes in Geo-Systems - Fundamentals, Modelling, Experiments and Applications*, vol. 2 of Elsevier Geo-Engineering Book Series, , pp. 181–186, Elsevier, 2004.

[16] L. Meng, T. Li, J. Xu, G. Chen, H. Ma, and H. Yin, "Deformation and failure mechanism of phyllite under the effects of THM coupling and unloading," *Journal of Mountain Science*, vol. 9, no. 6, pp. 788–797, 2012.

[17] Q. L. Ding, F. Ju, S. B. Song, B. Y. Yu, and D. Ma, "An experimental study of fractured sandstone permeability after high-temperature treatment under different confining pressures," *Journal of Natural Gas Science and Engineering*, vol. 34, pp. 55–63, 2016.

[18] D. W. Liu, Y. Liu, and C. H. Zhao, "Experimental study on the characteristics of permeability in the all failure process of mudstone," *Journal of Xi'an University of Science and Technology*, vol. 35, no. 1, pp. 78–82, 2015.

[19] G. Chen, T. Li, G. Zhang, H. Yin, and H. Zhang, "Temperature effect of rock burst for hard rock in deep-buried tunnel," *Natural Hazards*, vol. 72, no. 2, pp. 915–926, 2014.

[20] D. Zhang, G. Fan, L. Ma, and X. Wang, "Aquifer protection during longwall mining of shallow coal seams: a case study in the Shendong Coalfield of China," *International Journal of Coal Geology*, vol. 86, no. 2-3, pp. 190–196, 2011.

[21] G. Fan and D. Zhang, "Mechanisms of aquifer protection in underground coal mining," *Mine Water and the Environment*, vol. 34, no. 1, pp. 95–104, 2015.